

LETTER

Spectroscopic evidence for five-coordinated Ni in $\text{CaNiSi}_2\text{O}_6$ glass

LAURENCE GALOISY, GEORGES CALAS

Laboratoire de Minéralogie-Cristallographie, UA CNRS 09, Universités de Paris 6 et 7, 75252 Paris, France

ABSTRACT

NiK-edge EXAFS and XANES and optical absorption spectroscopy experiments have been performed on a $\text{CaNiSi}_2\text{O}_6$ glass. The data are consistent with the presence of ^{57}Ni in a trigonal bipyramidal symmetry site, a previously unknown surrounding. Minor amounts of ^{60}Ni are also present. This environment explains why the Ni-O distances derived from EXAFS in the glass are shorter than in the crystalline equivalent and provides a rationale for the high olivine/liquid partition coefficients of Ni that govern its preferential location in mafic and ultramafic rocks.

INTRODUCTION

Melt structure exercises an important control on mineral/melt trace-element partitioning (Mysen and Virgo, 1980). This control originates from the differences in the site energy of the elements in melts and minerals. In contrast to network-forming elements such as Si, which occur as tetrahedral species in silicate glasses at ambient pressure, the coordination of network modifier cations (e.g., transition elements) in glasses has long been a matter of debate. Among these transition elements, Ni is important for understanding the genesis of mafic and ultramafic magmas because of its high mineral/liquid partition coefficients (D) (Kinzler et al., 1990). Optical absorption spectra of Ni-bearing silicate glasses have been interpreted in terms of a coexistence of ^{41}Ni and ^{61}Ni (Burns and Fyfe, 1964; Calas and Petiau, 1983). However, as observed for other divalent transition elements in glasses (Calas and Petiau, 1983), the short Ni-O distances derived from extended X-ray absorption fine structure (EXAFS) are not compatible with ^{61}Ni .

We report here a comparative spectroscopic study of Ni coordination in crystalline and amorphous $\text{CaNiSi}_2\text{O}_6$ using either local symmetry-sensitive spectroscopic methods [optical absorption spectroscopy, X-ray absorption near edge fine structure (XANES)] or EXAFS that gives a partial distribution function (see Calas et al., 1987; Brown et al., 1988).

EXPERIMENTAL

A C2/c $\text{CaNiSi}_2\text{O}_6$ pyroxene synthesized according to the procedure of Navrotsky and Coons (1976) was melted by heating to about 1340 °C for 4 h in a Pt crucible and then quenched to a crystal-free glass by immersing the bottom of the crucible in H_2O . Electron probe microanalysis showed that the materials are chemically homogeneous with $\text{Ca}_{1.01}\text{Ni}_{0.87}\text{Si}_{2.06}\text{O}_6$ and $\text{Ca}_{1.01}\text{Ni}_{0.98}\text{Si}_{2.02}\text{O}_6$ for the glass and crystal, respectively. Diffuse-reflectance optical spectra were obtained using a 2300 CARY spectrophotometer fitted with an integrating sphere attach-

ment coated with halon. The reflectance R was obtained by reference to halon and converted into a remission function $F(R)$ (Cervelle and Maquet, 1982).

NiK-edge XAS transmission spectra were recorded on the EXAFS-4 station at the LURE DCI Synchrotron Radiation Facility (Orsay, France). The storage ring was operated at 1.85 GeV and 250 mA. Si 111 and Si 311 two-crystal monochromators were used for EXAFS and XANES measurements, respectively. XAS spectra of finely ground powders were collected at both room temperature and at 4.8 K and calibrated by reference to metallic Cu. EXAFS spectra were normalized using Victoreen and spline background-fitting functions and recalculated into k space (k represents the photoelectron momentum) by reference to a threshold energy E_0 ($E_0 = 8340$ eV). The Fourier transform (FT) of the k^3 -weighted EXAFS was computed using a Kaiser window over the k range of 3–12 Å^{-1} to minimize Fourier termination effects. EXAFS data reduction (see, e.g., Brown et al., 1988) was performed using theoretical phase shift and amplitude functions (McKale et al., 1988). The validity of these functions has been ensured for ^{41}Ni and ^{61}Ni in NiCr_2O_4 and $\text{Ni}(\text{OH})_2$, respectively. The interatomic distances $d(\text{Ni-O})$ and number of neighbors N are in agreement with the known structures, within 0.01 Å and 0.5, respectively. Values of $d(\text{Ni-O})$, N , and the Debye-Waller-like parameter σ together with the correction term ΔE_0 , which accounts for any inaccuracy in the threshold energy definition, have been refined using least-squares iteration, the mean free path parameter λ being held constant at 1.7 Å .

RESULTS

The EXAFS spectra of crystalline and glassy $\text{CaNiSi}_2\text{O}_6$ have distinctly different shapes (Fig. 1). The frequency of the oscillations is significantly lower in the glass compared with the crystal. The FT shows the various atomic shells contributing to the EXAFS in crystalline and glassy $\text{CaNiSi}_2\text{O}_6$ (Fig. 2). A prominent peak is observed at an apparent distance of 1.7 and 1.6 Å (uncorrected for phase

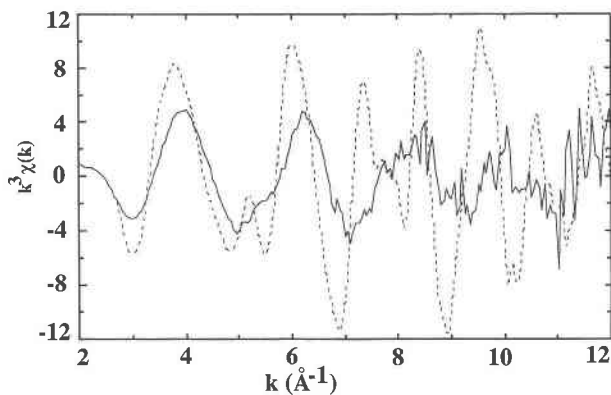


Fig. 1. NiK-EXAFS $k^3\chi(k)$ in crystalline (dashed line) and amorphous (solid line) $\text{CaNiSi}_2\text{O}_6$.

shift) in the crystal and glass, respectively, and it is broader and less intense in the latter. Fitting the back transform of this first major peak of the FT in the nickel pyroxene yielded structural data [$d(\text{Ni-O}) = 2.07 \pm 0.01 \text{ \AA}$ and $N = 5.8 \pm 0.5$] in good agreement with the known structure [$d(\text{Ni-O}) = 2.075 \text{ \AA}$ and $N = 6$, Ghose et al., 1987]. A further contribution is also found in the nickel pyroxene near 2.8 \AA and corresponds to the next-nearest cation neighbors. The Ni-O distances and number of neighbors are smaller in the glass than in the crystal [$d(\text{Ni-O}) = 1.98 \pm 0.01 \text{ \AA}$ and $N = 4.5 \pm 0.5$]. Only a residual peak is observed near 2.7 \AA in the FT, indicating a loss of medium-range order. EXAFS parameters for the Ni-O shell do not show a significant thermal dependence, σ varying from 0.106 \AA at 300 K to 0.090 \AA at 4.8 K in the glass and remaining constant at 0.083 \AA in the crystal.

The NiK-XANES spectra of the glass and the reference compounds are shown in Figure 3. The preedge intensity, relative to the average atomic absorption, as well as the shape, energy position, and relative intensity of the edge

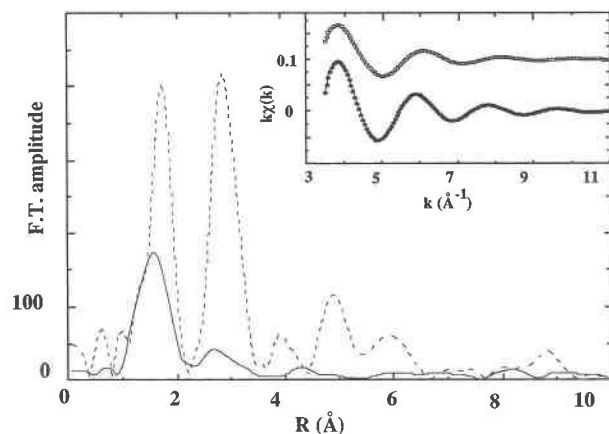


Fig. 2. Fourier transforms of $k^3\chi(k)$. Inset: calculated Fourier filtered $k^3\chi(k)$ spectrum for O coordination shell in the crystal (solid circles) and the glass (open circles). Dashed and solid lines are as in Figure 1.

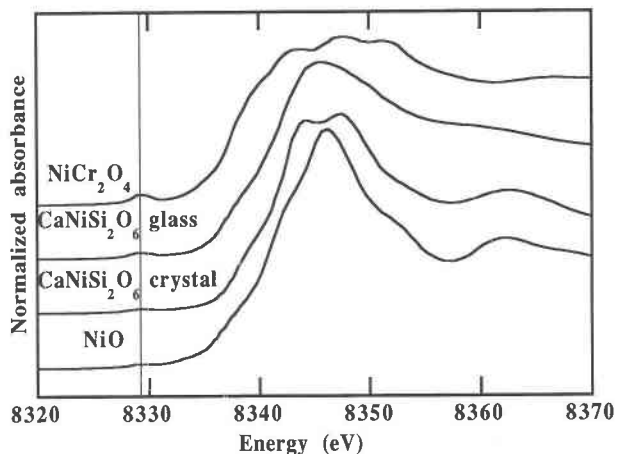


Fig. 3. NiK-XANES spectra calibrated by reference to metallic Cu. The intensity of the preedge (marked by the vertical solid line) relative to the average atomic absorption equals 0.023 in the glass as compared to 0.011, 0.015, and 0.045 in crystalline $\text{CaNiSi}_2\text{O}_6$, NiO, and NiCr_2O_4 , respectively.

crest observed in the glass are intermediate between those of ^{44}Ni and ^{60}Ni . The preedge intensity indicates the absence of an inversion center at the Ni site, as for other transition elements in glasses (Calas and Petiau, 1983; Waychunas et al., 1988). The shape of the main edge precludes a significant distortion of the site occupied by Ni in the glass as well as the presence of square planar complexes (Briois et al., 1989).

The optical absorption spectrum of the green $\text{CaNiSi}_2\text{O}_6$ pyroxene shows three main transitions (Fig. 4) at the same position as in other ^{60}Ni -bearing phases (Rossman et al., 1981; Manceau and Calas, 1985). Weaker absorptions near 20000 cm^{-1} result from forbidden transitions. In contrast to the crystal, the brown-colored glass shows five bands with different positions and relative intensities. The ^{44}Ni is responsible for the two shoulders near 15700 cm^{-1} and 18000 cm^{-1} . These transitions, if present, are always observed at the same position in oxide compounds (Galoisy et al., 1991) and correspond to the most intense split transition of ^{44}Ni [${}^3\text{T}_1(\text{F}) \rightarrow {}^3\text{T}_1(\text{P})$]. The low intensity of this transition indicates the presence of about 30% of ^{44}Ni . Two other bands of halved intensities are predicted for ^{44}Ni , near 5000 cm^{-1} and 8300 cm^{-1} , corresponding to the ${}^3\text{T}_1(\text{F}) \rightarrow {}^3\text{T}_2(\text{F})$ (crystal field) and ${}^3\text{T}_1(\text{F}) \rightarrow {}^3\text{A}_2(\text{F})$ transitions, respectively (Fig. 4). These transitions are included in the broad, unresolved band (full width, 4200 cm^{-1}) observed near 10700 cm^{-1} , which can be fitted by at least three Gaussian components, and in the narrow band (full width, 1500 cm^{-1}) observed near 5300 cm^{-1} . The two bands near 10700 cm^{-1} and 22000 cm^{-1} cannot arise from ^{60}Ni as their positions are outside what is usually observed in ^{60}Ni -bearing silicates (Rossman et al., 1981). Indeed, in ^{60}Ni , the energy of the transitions to the ${}^3\text{P}$ state is unaffected by splitting and remains in the range $23500\text{--}24500 \text{ cm}^{-1}$. However, it is observed at 22000 cm^{-1} in the glass. The same reasoning

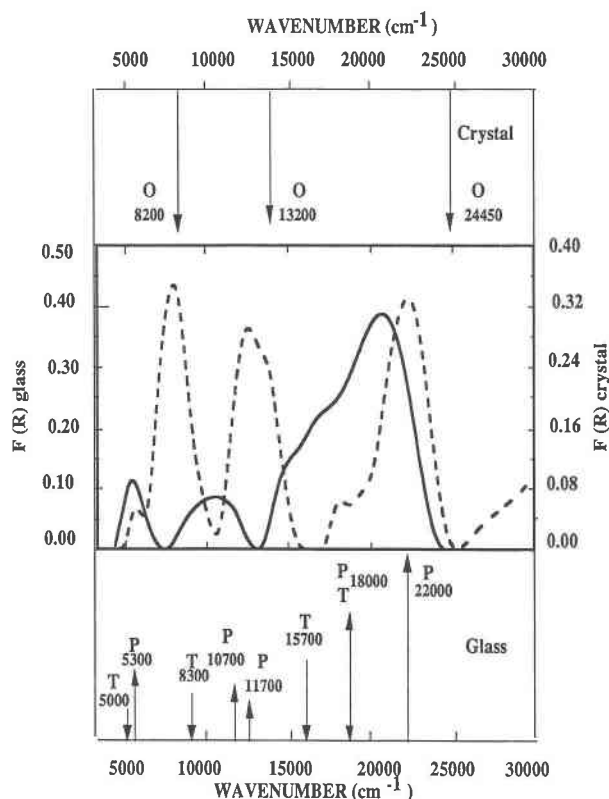


Fig. 4. Optical absorption spectra of crystalline (dashed line) and vitreous (solid line) $\text{CaNiSi}_2\text{O}_6$. The spectral attributions are indicated at the top and bottom for the crystal and glass, respectively. The position of the allowed electronic transitions is indicated in the following symmetries: O = ^{16}Ni , P = fivefold Ni (di-trigonal pyramid), T = ^{14}Ni .

holds for the transition near 10700 cm^{-1} as the crystal field transition in ^{16}Ni occurs in the range $7000\text{--}8500\text{ cm}^{-1}$. Even in the case of highly distorted surroundings such as the octahedral M2 sites of enstatite (Rossman et al., 1981), this transition is split into a component near 4300 cm^{-1} with the other component remaining near 8500 cm^{-1} .

DISCUSSION

XAS indicates a shortening of Ni-O distances in the glass as compared with the crystal, which is consistent with small coordination numbers, and no significant site distortion in either phase. On the other hand, most optical transitions in the glass are shifted toward low wavenumbers relative to those of ^{16}Ni , indicating larger Ni-O distances in the glass if ^{16}Ni is assumed. Consequently, there is an apparent disagreement between spectroscopic data. The previous interpretations of Ni optical spectra in glasses (Burns and Fyfe, 1964; Nelson et al., 1983) are thus not satisfactory. A new coordination state of Ni^{2+} in glasses has to be sought.

The position of the levels derived from the ^3P atomic state depends largely on covalency factors. In ^{16}Ni , a po-

sition at high wavenumbers ($23500\text{--}25000\text{ cm}^{-1}$) may be accounted for by ionic Ni-O bonds. When Ni is fourfold coordinated, the decrease by about 20% of the ^3P state arises from an enhanced Ni-O covalent bonding. In the glass, the position of this transition at about 22000 cm^{-1} may be explained by an intermediate covalency. This and the fact that no crystal field transitions corresponding to ^{16}Ni may be observed at this value, ^{15}Ni is suspected. The assignment of the bands observed in the glass is in good agreement with ^{15}Ni located in a trigonal bipyramidal (TBP) site (Morassi et al., 1973) with a crystal field energy of 10700 cm^{-1} [transition $^3\text{E}'(\text{F}) \rightarrow ^3\text{A}_2''(\text{F})$, $^3\text{A}_2''(\text{F})$] (Fig. 3). As shown in Figure 2, the bands at 5300 cm^{-1} [$^3\text{E}'(\text{F}) \rightarrow ^3\text{E}''(\text{F})$], 22000 cm^{-1} [$^3\text{E}'(\text{F}) \rightarrow ^3\text{A}_2(\text{P})$], and 10700 cm^{-1} correspond to transitions of ^{15}Ni . Two other transitions are predicted for this coordination geometry at 11700 cm^{-1} [$^3\text{E}'(\text{F}) \rightarrow ^3\text{A}_2(\text{F})$] and 18000 cm^{-1} [$^3\text{E}'(\text{F}) \rightarrow ^3\text{E}'(\text{P})$]. The transitions arising from ^{14}Ni in the glass (see above) at about 5000 cm^{-1} and 18000 cm^{-1} are superimposed with those of ^{15}Ni , which explains the absence of apparent splitting of these bands. The ^{15}Ni is also consistent with glass XANES features, e.g., the high preedge intensity (Briois et al., 1989).

EXAFS-derived Ni-O mean distances and the Ni mean coordination number are smaller in the glass than in the crystal. The Ni-O distances corresponding to ^{14}Ni and ^{15}Ni [about 1.95 \AA and $1.98\text{--}2\text{ \AA}$ (Lyutin et al., 1973), respectively] cannot be distinguished with the accuracy of EXAFS, especially if possible site variations among the compounds are taken into account. A mixture of ^{15}Ni (TBP) and ^{14}Ni explains the number of neighbors found in the glass. Because of the similarity of the Ni-O distances in both coordinations, σ values are not expected to increase significantly in such a distribution (Eisenberger and Brown, 1979). At 4.8 K , σ depends mostly on static radial disorder. The $\sigma^2/d(\text{Ni-O})$ ratio ($3.3 \times 10^{-3}\text{ \AA}$ and $4.1 \times 10^{-3}\text{ \AA}$ for the crystal and glass, respectively) is lower than 10^{-2} \AA and shows that the harmonic model is valid. The absence of significant local disorder is confirmed by the fact that the optical Gaussian components of the glass spectrum are not broadened compared with the crystal.

This study points out a coordination number smaller in the glass than in the crystalline counterpart. This property appears to be a characteristic of glass structure (Calas et al., in preparation), as it is found for most network modifiers (e.g., Ca, Eckersley et al., 1988) or transition elements (e.g., Mn, Fe, or Co; Calas and Petiau, 1983; Waychunas et al., 1988). Though not usually encountered in crystalline silicates, pentahedral coordination has recently been evidenced in silicate glasses (see, e.g., Stebbins and McMillan, 1989). If the glasses are considered as instantaneous images of the melt structure, the difference observed in the element surroundings between minerals and silicate glasses/melts might be the driving force for element distribution during magma crystallization. In the specific case of Ni, the octahedral site-preference energy is the origin for the high olivine/liquid partition co-

efficients, as Ni is found in octahedral sites in olivines and not in the glasses/melts. This prediction is consistent with the experimental observations (Kinzieler et al., 1990), which explains the preferential location of Ni in mafic and ultramafic rocks. A similar mechanism has been suggested earlier by Burns and Fyfe (1964) by considering coexisting ⁶³Ni and ⁶⁴Ni in the silicate glasses/melts. It thus bears a more general significance in the absence of any ⁶³Ni in silicate glasses.

ACKNOWLEDGMENTS

We thank G.E. Brown, Jr. and an anonymous reviewer for their helpful comments on this paper and P.H. Gaskell for fruitful discussions. We are grateful to Aline Ramos and the staff of LURE (Orsay) for their help in XAS measurements. This work was supported by the CNRS/INSU DBT Cooperative Program (Contribution CNRS/DBT no. 89-357).

REFERENCES CITED

- Briois, V., Cartier, C., Momenteau, M., Maillard, Ph., Zarembowitch, J., Dartyge, E., Fontaine, A., Tourillon, G., Thiéry, P., and Verdager, M. (1989) Spectroscopie d'absorption des rayons X au seuil K: Complexes moléculaires du cobalt. *Journal de Chimie Physique*, 86, 1623–1634.
- Brown, G.E., Jr., Calas, G., Waychunas, G.A., and Petiau, J. (1988) X-ray absorption spectroscopy: Applications in mineralogy and geochemistry. In *Mineralogical Society of America Reviews in Mineralogy*, 18, 431–512.
- Burns, R.G., and Fyfe, W. (1964) Site of preference energy and selective uptake of transition-metal ions from a magma. *Science*, 144, 1001–1003.
- Calas, G., and Petiau, J. (1983) Structure of oxide glasses. Spectroscopic studies of local order and crystallochemistry. *Geochemical implications*. *Bulletin de Minéralogie*, 106, 33–55.
- Calas, G., Brown, G.E., Jr., Waychunas, G.A., and Petiau, J. (1987) X-ray absorption spectroscopic studies of silicate glasses and minerals. *Physics and Chemistry of Minerals*, 15, 19–29.
- Cervelle, B., and Maquet, M. (1982) Cristallographie des lizardites substituées Mg-Fe-Ni par spectrométrie visible et infrarouge proche. *Clay Minerals*, 17, 377–392.
- Eckersley, M.C., Gaskell, P.H., Barnes, A.C., and Chieux, P. (1988) Structural ordering in a calcium silicate glass. *Nature*, 335, 525–527.
- Eisenberger, P., and Brown, G.S. (1979) The study of disordered systems by EXAFS: Limitations. *Solid State Communications*, 29, 481–484.
- Galoisy, L., Calas, G., and Maquet, M. (1991) Alumina fused cast refractory ageing monitored by nickel crystal chemistry. *Journal of Materials Research*, 6, in press.
- Ghose, S., Wan, C., and Okamura, F.P. (1987) Crystal structures of CaNiSi₂O₆ and CaCoSi₂O₆ and some crystal-chemical relations in C2/c clinopyroxenes. *American Mineralogist*, 71, 375–381.
- Kinzieler, R.J., Grove, T.L., and Recca, S.I. (1990) An experimental study on the effect of temperature and melt composition on the partitioning of nickel between olivine and silicate melt. *Geochimica et Cosmochimica Acta*, 54, 1255–1265.
- Lyutin, V.I., Tutov, A.G., Llyukhin, V.V., and Belov, N.V. (1973) Crystal structure of the antiferromagnetic K₂Ni phosphate KNiPO₄. *Soviet Physics Doklady*, 18, 12–14.
- Manceau, A., and Calas, G. (1985) Heterogeneous distribution of nickel in hydrous silicates from New Caledonia ore deposits. *American Mineralogist*, 70, 549–558.
- McKale, A.G., Veal, B.W., Paulikas, A.P., Chan, S.K., and Knapp, G.S. (1988) Improved ab initio calculations of amplitude and phase functions for extended X-ray absorption fine structure spectroscopy. *Journal of the American Chemical Society*, 110, 3763–3768.
- Morassi, R., Bertini, I., and Sacconi, L. (1973) Five coordination of iron (II), cobalt (II) and nickel (II) complexes. *Coordination Chemistry Reviews*, 11, 343–402.
- Mysen, B.O., and Virgo, D. (1980) Trace element partitioning and melt structure: An experimental study at 1 atm pressure. *Geochimica et Cosmochimica Acta*, 44, 1917–1930.
- Navrotsky, A., and Coons, W.E. (1976) Thermochemistry of some pyroxenes and related compounds. *Geochimica et Cosmochimica Acta*, 40, 1281–1288.
- Nelson, C., Furukawa, T., and White, W.B. (1983) Transition metal ions in glasses: Network modifiers or quasi-molecular complexes? *Materials Research Bulletin*, 18, 959–966.
- Rossman, G.R., Shannon, R.D., and Waring, R.K. (1981) Origin of the yellow color of complex nickel oxides. *Journal of Solid State Chemistry*, 39, 277–287.
- Stebbins, J.F., and McMillan, P. (1989) Five- and six-coordinated Si in K₂Si₄O₈ glass quenched from 1.9 GPa and 1200 °C. *American Mineralogist*, 74, 965–968.
- Waychunas, G.A., Brown, G.E., Ponader, C.W., and Jackson, W.E. (1988) Evidence from X-ray absorption for network-forming Fe²⁺ in molten silicates. *Nature*, 332, 251–253.

MANUSCRIPT RECEIVED JUNE 21, 1991

MANUSCRIPT ACCEPTED AUGUST 6, 1991